San Jose State University

SJSU ScholarWorks

Faculty Research, Scholarly, and Creative Activity

4-19-2019

Induced quantum dot probe for material characterization

Yun-Pil Shim
University of Maryland

Rusko Ruskov
University of Maryland

Hilary M. Hurst
Laboratory for Physical Sciences, hilary.hurst@sjsu.edu

Charles Tahan
Laboratory for Physical Sciences

Follow this and additional works at: https://scholarworks.sjsu.edu/faculty_rsca

Part of the Quantum Physics Commons

Recommended Citation

Induced quantum dot probe for material characterization

Yun-Pil Shim, Rusko Ruskov, Hilary M. Hurst, and Charles Tahan

COLLECTIONS

F This paper was selected as Featured

SCI This paper was selected as Scilight

View Online   Export Citation   CrossMark

ARTICLES YOU MAY BE INTERESTED IN

Reconfigurable spin logic device using electrochemical potentials
Applied Physics Letters **114**, 152403 (2019); https://doi.org/10.1063/1.5089274

A quantum engineer's guide to superconducting qubits
Applied Physics Reviews **6**, 021318 (2019); https://doi.org/10.1063/1.5089550

Proposed probe chip a potential shortcut for quantum device manufacturing cycle
Scilight **2019**, 160003 (2019); https://doi.org/10.1063/1.5100278

Induced quantum dot probe for material characterization SCI F

View Online   Export Citation   CrossMark

Yun-Pil Shim,[1,2] (iD) Rusko Ruskov,[1,2] Hilary M. Hurst,[1] and Charles Tahan[1,a]

AFFILIATIONS

[1]Laboratory for Physical Sciences, College Park, Maryland 20740, USA
[2]Department of Physics, University of Maryland, College Park, Maryland 20742, USA

[a]Electronic mail: charlie@tahan.com

ABSTRACT

We propose a non-destructive means of characterizing a semiconductor wafer via measuring the parameters of an induced quantum dot on the material system of interest with a separate probe chip that can also house the measurement circuitry. We show that a single wire can create the dot, determine if an electron is present, and be used to measure critical device parameters. Adding more wires enables more complicated (potentially multi-dot) systems and measurements. As one application for this concept, we consider a silicon metal-oxide-semiconductor and silicon/silicon-germanium quantum dot qubits relevant to quantum computing and show how to measure low-lying excited states (so-called "valley" states). This approach provides an alternative method for the characterization of parameters that are critical for various semiconductor-based quantum dot devices without fabricating such devices.

Published under license by AIP Publishing. https://doi.org/10.1063/1.5053756

Semiconductor heterostructures often serve as the substrate for many solid-state devices. For quantum devices such as qubits, their quality depends crucially on the properties of these wafers. Often, these qubit characterization parameters can only be ascertained by fabricating the device and measuring it at cryogenic temperatures. Quantum dots (QDs) in silicon for quantum computing (QC)[1] are a great example. The indirect band-gap of silicon creates low-lying excited (valley) states in the QD heterostructure; if the "valley splitting" is too small, initialization, readout and even gate operation of the qubits are impeded. Optimizing the valley splitting of silicon QD qubits—in addition to other important parameters such as coherence time, charge noise, etc.—is needed for the eventual construction of quantum computers, and is limited by the design-fabrication-test cycle time.

We propose a method for characterizing material properties using a separate probe chip that both creates the dot(s) and measures them. This concept was inspired by the ion trap stylus approach,[2,3] where an ion qubit is trapped on a stylus-like tip that can be brought close to a material to characterize its properties, and also by the scanning nitrogen-vacancy (NV) center tip which can be used to detect magnetic fields on a nanoscale for imaging or to couple to spin qubits.[4] While these ideas involve putting a qubit on the scanning tip itself, our scheme uses a separate *gate chip* to *induce* a qubit in the material structure under study, then measure those material and qubit parameters of interest using the circuits on the gate chip. Indeed, scanning tunneling

microscope (STM) tips have already been used to create effective dots on the surface of InAs[5,6] and, more recently, Si,[7] using tunneling to perform spectroscopy. Nondestructive characterization of embedded donor atoms in a semiconductor has also been demonstrated using a scanning tip architecture.[8,9] Here, we induce the dot qubit within the material in an environment realistic to quantum computing and consider dispersive readout for characterizing material and qubit properties.

To justify the viability of our approach, we specifically consider silicon metal-oxide-semiconductor (MOS) type and silicon/silicon-germanium quantum well (QW) type structures as examples to investigate the relevant properties of silicon-based qubit devices. We describe the general geometry of the heterostructure wafer and the gate chip and provide electrostatic simulations of the induced QD. Then, we show how to load the QD and detect the electron by a dispersive readout using the quantum capacitance of the induced QD all with the same wire. Finally, methods for measuring the valley splitting based on a much stronger quantum capacitance of the qubit levels at spin-valley anticrossing are discussed using one or more wires.

Figure 1 shows schematic pictures of a possible setup. The gate chip containing the required trapping and the measurement circuitry is placed perpendicular above a semiconductor structure, such as a MOS [Fig. 1(a)] or Si/SiGe QW structure [Fig. 1(b)]. Applying a positive voltage V_g to the gate wire induces a confining electrostatic
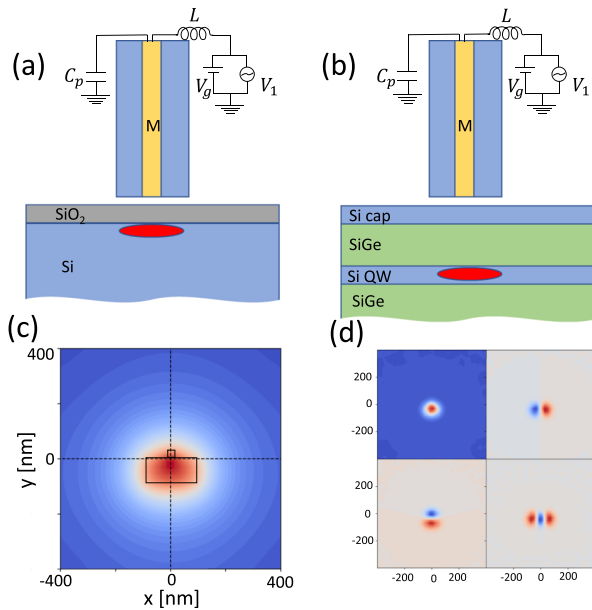
FIG. 1. Schematic diagram of the device, for MOS (a) and QW (b) structures. A Si wafer chip with a metallic gate wire M on it (and other necessary circuitry; L is the inductance and C_p is the unavoidable parasitic capacitance) is positioned above the semiconductor heterostructure to induce a QD for non-invasive characterization. DC and AC voltages can be simultaneously applied to the gate wire for inducing the quantum dot and its characterization. Wire induced QD confining potential and four lowest orbitals, $\mathrm{Re}[\psi_i]$, in a MOS device with a DC gate voltage $V_g = 0.02$ V are shown in (c) and (d), respectively.

potential in the 2D quantum well in the structure [Fig. 1(c)], and orbital wavefunctions ψ_i show typical 2D QD orbital characters [Fig. 1(d)]. Electrons can be trapped into the induced QD, as is depicted by red regions in Fig. 1(a) for the MOS and Fig. 1(b) for the QW. The energy levels of the induced QDs have nonzero second derivative with respect to the applied voltage (i.e., a quantum capacitance), allowing for a dispersive readout by coupling to a detector circuit which can be integrated in the gate chip.[10–13]

We performed electrostatic simulation of the device[14] using dimensions for MOS and QW devices that are typically used in experiments. For a MOS structure,[15–18] a silicon oxide layer of 10 nm overlays the silicon substrate of $\gtrsim 200$ nm. For a QW structure,[19,20] a strained silicon quantum well of 10 nm is sandwiched between a $\gtrsim 200$ nm SiGe substrate and a 40 nm SiGe spacer which is capped by 10 nm of silicon. We choose a reasonable and manufacturable gate chip design to demonstrate the main concepts in this work. The gate wire size is chosen to be 10 nm × 10 nm and 1 μm long, and 10 nm away from the top of the heterostructure. We considered different sizes of gate wafers as well as a bare metallic wire tip with no gate wafer for the simulations and obtained qualitatively similar results. To be specific, we present below the results for the gate wire on a silicon wafer of 100 nm depth and 200 nm width.

To conduct measurements of useful device properties, especially for properties relevant for spin qubits, we need to populate the induced quantum dot with a controlled number of electrons. This can be achieved in a number of different ways: e.g., (i) an electron-hole pair

can be generated near the induced QD by light, and the electron is trapped into the QD, while the hole is pushed away from the QD by the electrostatic force, or (ii) one can dope the semiconductor by implanting donors in a specific region (or use a large "electron bath" gate[10,12]) and use the dot accumulation wire to load electrons from the doped region into the QD (one could then possibly move the electron to another area on the chip as in the STM induced QD device[7]). Once isolated, the dot gate voltage can be tuned to enhance the quantum capacitance while maintaining single occupation.

We can detect the charge in the QD via dispersive readout[10–13] by incorporating a tank-circuit (often superconducting) resonator (typically with a frequency ω_r of a few hundred megahertz to a few gigahertz) into the gate wire and accumulated QDs [e.g., Fig. 1(a)], and then sending and reflecting resonant microwaves into it. There would be no phase shift of the reflected signal from an empty dot, but if there is a trapped electron, the reflected signal will be phase shifted if the quantum capacitance[21–27] of the electron energy level is large enough. We send an rf-signal (along with the DC voltage V_g): $V = V_g + V_1 \cos(\omega_r t)$. In addition to the conventional capacitance of the gate-to-heterostructure QD, C_{MOS}, and a distributed parasitic capacitance C_p of the gate to the ground plane, as is depicted in Figs. 1(a) and 1(b), there will be a quantum capacitance $C_{q,i} = \alpha_c^2 \frac{\partial^2 E_i}{\partial V_g^2}$ of the induced QD, including the lever arm $\alpha_c \equiv \frac{C_c}{C_c + C_d}$ of the tip-to-dot capacitive coupling (here, C_c and C_d are the tip-to-dot and dot-to-ground capacitances, respectively; for further estimations, we assume $\alpha_c \sim 1$). The quantum capacitance arises from the non-linear voltage response of the QD's energy levels,[27] $E_i(V_g) = E_i(V_g^0) + \frac{\partial E_i}{\partial V_g} \delta V_g + \frac{1}{2} \frac{\partial^2 E_i}{\partial V_g^2} \delta V_g^2$, assuming slow in time voltage perturbation δV_g. It leads to a frequency shift of the tank-circuit,[27] and the corresponding phase shift of the reflected signal due to C_q would be[10,11]

$$\Delta \phi \simeq Q \frac{\delta C}{C_{\mathrm{tot}}} \equiv Q \frac{C_q}{C_p + C_{\mathrm{MOS}} + C_q}, \qquad (1)$$

where the Q-factor is defined via the tank-circuit relaxation $\kappa = \omega_r/Q$. [For a single QD level, the non-linear voltage response arises from the spatial change of the orbitals, which is often neglected in Hubbard-like Hamiltonians. We recently showed the differences between a Hubbard-like Hamiltonian and the actual induced QD system, and its consequences on QD devices.[28]] Figs. 2(a) and 2(b) show the QD confining potentials at various V_g values for the MOS and QW devices, respectively. The second derivative of the orbital energy levels with respect to the applied V_g is shown in Fig. 2(c) for the MOS and Fig. 2(d) for the QW. The absolute value of the quantum capacitance is larger for a smaller gate voltage V_g and can be as large as $\lesssim 0.03$ aF for the MOS and $\lesssim 0.01$ aF for the QW at $V_g = 0.02$ V, for the geometry studied in this work.

For typical low Q tank-circuits[10,12] having C_{tot} of a few hundred femtofarads (and a frequency in the few hundred megahertz range), a capacitance change at a level of a few attofarads is measurable,[12] leading to a phase shift $\Delta \phi \approx 10^{-4}$–$10^{-5}$. Figures 2(e) and 2(f) show the calculated phase shift for $C_{\mathrm{tot}} = 1000$ fF, vs Q and V_g from Eq. (1) (assuming $\frac{\delta C}{C_{\mathrm{tot}}} \ll 1/Q$). The sensitivity to measure a small quantum capacitance will increase for moderately large tank-circuit Q-factors (e.g., the recently proposed high-kinetic inductance nano-wire resonators[29] with a frequency of a few gigahertz, and $Q \approx 10^3$ can be used in
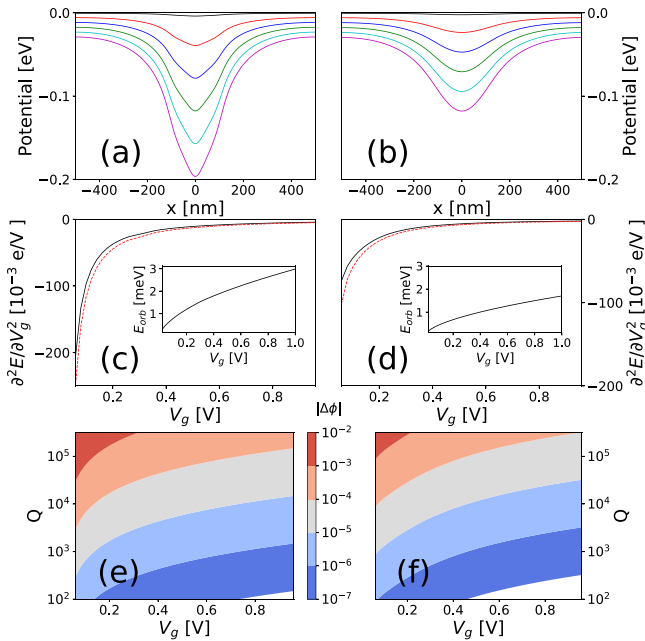
FIG. 2. Simulation of the induced QD potential and energy levels' quantum capacitance, $\partial^2 E_i / \partial V_g^2$. (a) QD potential on a MOS device, for various gate voltages $V_g = 0.02, 0.2, 0.4, 0.6, 0.8,$ and 1.0 V from top to bottom. (b) QD potential of the Si/SiGe QW device, for the same V_g values. (c) and (d) are the quantum capacitances of the two lowest energy levels of the induced QD for MOS and QW structures, respectively. The solid black (dashed red) curves indicate the ground (first excited) orbitals. Insets show the energy splitting between the two lowest orbitals vs the applied gate voltage V_g. (e) and (f) show the calculated phase shift, $\Delta\phi$, of the reflected signal as a function of the voltage V_g and the quality factor Q of the resonator circuit for the MOS and QW devices, respectively, assuming that the induced dot is singly occupied.

our proposed vertical gate circuit). As an example, for $C_q \gtrsim 0.01$ aF as per the simulation, and a reachable resonator parameter:[29] $C_{tot} \approx 30$ fF, $Q \approx 10^3$, one can obtain $\Delta\phi \gtrsim 3 \times 10^{-4}$, which is readily measurable.[11,12] The lowest detectable C_q may be limited by unwanted variation in the gate-to-QD capacitance as a function of gate voltage (e.g., due to interface traps below the QD gate[12]).

If the device is in a configuration where the induced QD is close to an electron reservoir or another quantum dot, then the charge stability diagram can be mapped out directly using the tunneling capacitance,[24] where the response signal peaks at a charge transition (similar to Ref. 10).

As an example of critical material parameters that the separate gate chip could measure, we now discuss how to measure the valley splitting in a silicon wafer. We first examine the case of a single QD with one electron. Following the ideas of Ref. 15, a relatively small accumulation mode QD as in Ref. 12 can ensure that the orbital splitting is much larger than the valley splitting, $E_{orb} \gg E_{VS}$, which allows us to consider only the lowest orbital states in the following analysis. Experimentally, $E_{VS} = 300$–800 μeV and $E_{orb} = 2$–8 meV in small QDs in a MOS device[15] and also $E_{VS} = 80$–100 μeV and $E_{orb} = 0.5$ meV in another MOS device.[30] For Si/SiGe quantum dots, E_{VS} could be of the order of 80–100 μeV, or it could be much smaller. In the simulation of

induced dots, the above is satisfied as E_{orb} is of the order of millielectronvolts [see insets of Figs. 2(c) and 2(d)].

The valley splitting, $E_{VS} \propto a V_g$, depends linearly on the applied top gate voltage.[15] By applying an in-plane magnetic field, the lowest two valley states are Zeeman splitting (with energy splitting E_Z into 4 levels, as is shown in Fig. 3(a). Levels 2 and 3 (with different valley content) anti-cross when $E_Z = E_{VS}$, which leads to levels' energy curvature with respect to the gate voltage V_g. Indeed, the splitting at anti-crossing, $\Delta_a \propto |r_{v1,v2}| E_{VS} (\beta_D - \alpha_R)$, can be phenomenologically parameterized with an (intervalley) dipole matrix element $r_{v1,v2}$,[15,31] implying a charge re-distribution as a result of interface-induced intervalley tunneling and spin-orbit couplings.[32] We have estimated[15] $\Delta_a = 10^{-4}$–10^{-3} E_{VS}, using a Rashba/Dresselhaus spin-orbit interactions, α_R, β_D, induced at the heterostructure interface.[32] Levels 2 and 3 then read: $E_{2,3}(V_g) = \frac{1}{2}[E_{VS}(V_g) \mp \sqrt{(E_{VS}(V_g) - E_Z(B))^2 + \Delta_a(V_g)^2}]$. This was used to describe the relaxation "hot spot" observed in the experiment, which is mainly due to acoustic phonon emission.[15]

Given this explicit level structure, we calculate the curvature of the levels with respect to the gate voltage V_g, obtaining the levels' quantum capacitances, $C_{q,i}$ (this quantifies the nonlinear response of the QD system[27]). In the magnetic field at anti-crossing [Fig. 3(a)], these quantum capacitances may be strongly enhanced with respect to those of the simple orbitals discussed above. The ground state has zero curvature ($C_{q,1} = 0$) from this effect, while for levels 2 and 3, one gets $C_{q,2} = -C_{q,3}$, and

$$C_{q,3} \simeq \frac{a^2}{2\Delta_a} \Bigg/ \left[\left(\frac{E_{VS} - E_Z}{\Delta_a}\right)^2 + 1\right]^{3/2}, \qquad (2)$$

with the capacitances sharply peaked near the anti-crossing (using a simple model with a linear dependence on V_g for the valley splitting[32]). With the experimentally estimated Δ_a and the valley splitting slope,[15] $a_{exp} \simeq 0.64$ meV/V, we obtain (for $E_{VS} = 100$ μeV) $|C_{q,2,3}| \simeq 0.3$ -3 aF, which should be measurable in experiments.[11,12] Another capacitance contribution may appear due to fast relaxation processes.[26] While the relaxation rate Γ_{rel} strongly increases at the spin-valley anti-crossing for a single electron QD[15] (reaching 10^7–10^8 s^{-1}),
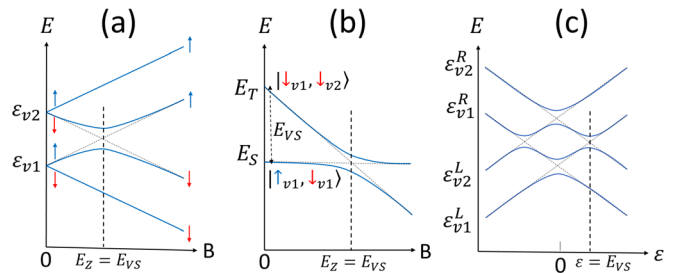
FIG. 3. Schematic QD energy levels for valley splitting measurement. (a) A QD with a single electron in an external magnetic field. The spin-valley states have a Zeeman splitting E_Z, and when it is equal to the valley splitting E_{VS}, there is an anti-crossing between the second and third levels. The energy curvature with respect to the gate voltage V_g is maximal at the anticrossing [Eq. (2)], since $\frac{\partial^2 E_i}{\partial V_g^2} \propto \frac{\partial^2 E_i}{\partial B^2}$ for the regime considered. (b) A QD with two electrons in it has singlet and triplet states, which anti-cross at $E_Z = E_{VS}$. (c) A DQD with a single electron has anti-crossings vs dots' detuning ε, related to electron tunneling with (without) conservation of valley index.

it is much slower than the chosen tank-circuit frequencies, $\Gamma_{\text{rel}} \ll \omega_r$, thus suppressing this capacitance contribution.[26] A way to enhance $|C_{q,2,3}|$ is to use the in-plane magnetic field with an angle such that Δ_a becomes much smaller;[32] however, making Δ_a smaller will narrow the region where C_q is significantly nonzero.

By scanning (sweeping) the magnetic field, we will register a sharp peak of phase change of the reflected signal when the Zeeman splitting is $E_Z = E_{\text{VS}}$. For this to work, we need to populate the excited states by choosing a temperature comparable to the valley splitting, e.g., for $E_{\text{VS}} = 100\ \mu\text{eV}$, the temperature should be $T \approx 1\ \text{K}$. Since $E_{\text{VS}} \gg \Delta_a$, the populations of levels 2 and 3 in Fig. 3(a) will be comparable, thus leading to an effective quantum capacitance suppression by $\Delta_a/kT \sim \Delta_a/E_{\text{VS}} \sim 10^{-3}$.

A way to mitigate these effects would be to use a single QD with two electrons. As shown in Fig. 3(b), the lowest two levels now anti-cross at $E_Z = E_{\text{VS}}$ with an anti-crossing splitting $\Delta_a^{2e} \approx \Delta_a$ (scf. Ref. 15), and the quantum capacitance is the same as in the 1-electron case, while the relaxation is strongly suppressed at anti-crossing. Also, the suppression effect due to temperature will not be as strong as in the 1-electron case, since $kT \sim \omega_r \lesssim 1\ \text{GHz}$ and so $\Delta_a/kT - \Delta_a/\omega_r \sim 10^{-1} - 10^{-2}$. However, since we are in a regime $\omega_r \gg \Delta_a$ (opposite to that where a quantum capacitance approximation is valid), the effective quantum capacitance is suppressed by a form factor: $C_{q,\text{eff}} \simeq C_q (\Delta_a/\omega_r)^2$. For example, for $E_{\text{VS}} \lesssim 100\ \mu\text{eV}$, the suppression factor is $(\Delta_a/\omega_r)^2 \approx 1/40^2$. Thus, this method would be sufficient to measure not too small valley splitting.

An alternative method to measure the valley splitting with a slightly more complicated gate circuit is to induce a double QD using two or three gate wires on the gate chip. Let us consider a DQD with a single electron, assuming each QD has the same valley splitting. The detuning between the QDs can be changed by tuning the voltages on the two QD-defining gates. At zero detuning ($\varepsilon = 0$), one is at the degeneracy point of the lower eigenvalley $v1$-electrons. [$v1$ is the lower valley and $v2$ is the upper valley state. See Fig. 3(c)]. The left-right tunneling t between the dots defines the splitting at anti-crossing, $2t$. One can then measure the change in the reflected signal at the degeneracy point (where the energy curvature is maximal) using a tank-circuit frequency $\omega_r \ll 2t$. By sweeping the detuning to $\varepsilon = E_{\text{VS}}$, the $v1$-electron from the left can tunnel to the $v2$-level from the right. This tunneling possibility forms another anti-crossing and the corresponding splitting (assuming the same $2t$). (This kind of tunneling is briefly discussed in Ref. 30 and then at length in Ref. 33.)

To measure the valley splitting, one starts at $\varepsilon = 0$ and populates the lowest two levels by temperature. One then moves (faster than the relaxation time T_1) to a detuning $\varepsilon = E_{\text{VS}}$, while sending a microwave with $\omega_r \ll 2t$, to encounter a sharp change in the reflected phase (provided that $t \ll E_{\text{VS}}$). This can be fulfilled for $2t \approx 2–4\ \text{GHz}$ and $\omega_r \approx 0.5–1\ \text{GHz}$. Once $\varepsilon = E_{\text{VS}}$ is reached, the reflected signal changes accordingly, due to the maximal quantum capacitance $C_q = e^2/2t$ similar to the experiment of Pettersson et al.[24] The quantum capacitance at this anti-crossing is estimated of the order of $10\ \text{fF}$, which is several orders of magnitude larger than at the spin-valley anti-crossing discussed above. In order to be able to distinguish the anti-crossings at $\varepsilon = 0$ and at $\varepsilon = E_{\text{VS}}$, one needs $E_{\text{VS}} \gtrsim 2t$ which sets the lowest measurable valley splitting, $E_{\text{VS}} \gtrsim 5 - 10\ \mu\text{eV}$. The main difference in this proposal from that of Ref. 33 is that the probing signal is far off resonance with the level splitting, at a constant tank-circuit frequency ω_r

$\ll 2t$, and the signature of valley splitting is easier to measure. These last two cases—a doubly occupied single QD and a singly occupied DQD—may be the easiest to experimentally implement as a first verification of this proposed methodology.

Finally, we note that an additional (tunable) microwave field can be introduced to the above proposed experiments to drive transitions between quantum dot states, which may allow for further or improved characterization (and also introduces another absolute energy scale to compare to, in addition to the magnetic field).

The proposal presented in this paper requires a sensitive measurement of small (quantum) capacitance changes, C_q, in the subatto-farad to attofarad range. The signal due to C_q may be obscured, however, in the presence of noise of large fluctuating capacitances, C_{MOS}, C_p (see Fig. 1). For example, fluctuations via the voltage dependence of $C_{\text{MOS}} (V_g)$ are attributed to the charging of interface traps below the QD gate;[12] the corresponding noise variation would be $\Delta C_{\text{MOS}}^{\text{noise}} = \left| \frac{\partial C_{\text{MOS}}}{\partial V_g} \right| \sqrt{\frac{S_V}{2t_{\text{av}}}}$, where S_V is the voltage spectral density and t_{av} is the averaging time. It was experimentally shown that below a sample-specific voltage threshold, $V_g < V_{\text{th}}$, the capacitance derivative was small, and a capacitance change of $\approx 1.5\ \text{aF}$ was resolved.[12] Another type of noise may enter through mechanical fluctuations of the tip. See e.g., experiments by Scanning Microwave Microscopy (SMM).[9,34] In an experiment of near-field SMM,[34] the (slow) resonator frequency fluctuations are tracked and stabilized via a feedback loop allowing a longer averaging time to reduce the noise; a sensitivity of $(0.06\ \text{aF})^2/\text{Hz}$ was limited by mechanical noise.[34] Since in our proposed experiment the tip is not moving, the mechanical noise may be reduced, eventually allowing for valley splitting measurement via a tip-induced QD in the Si heterostructure.

Inducing quantum dots instead of fabricating them offers potential for nondestructive characterization either locally or across a wafer, speeding the optimization of materials and quantum devices such as qubits. Our concept is applicable to other materials and systems as the inducing and measurement chips can be fabricated on a substrate different from the materials system under consideration. We show that inducing QDs and measuring valley splitting in silicon devices are plausible with the current experimental technology. Induced QD devices and the actual quantum devices built on the wafer will be different, but they share many critical aspects of the underlying material. Characterization of the induced QD devices will provide useful information of the yet-to-be-built devices. Based on this concept, other materials and systems (germanium, holes instead of electrons, topological systems, etc.) and qubit approaches (encoded qubits, different readout techniques, and even linear arrays of qubits making small quantum computers) can be explored without actually fabricating the quantum dots themselves.

REFERENCES

[1] F. A. Zwanenburg, A. S. Dzurak, A. Morello, M. Y. Simmons, L. C. L. Hollenberg, G. Klimeck, S. Rogge, S. N. Coppersmith, and M. A. Eriksson, Rev. Mod. Phys. **85**, 961 (2013).

[2] R. Maiwald, D. Leibfried, J. Britton, J. C. Bergquist, G. Leuchs, and D. J. Wineland, Nat. Phys. **5**, 551 (2009).

[3]C. L. Arrington, K. S. McKay, E. D. Baca, J. J. Coleman, Y. Colombe, P. Finnegan, D. A. Hite, A. E. Hollowell, R. Jördens, J. D. Jost, D. Leibfried, A. M. Rowen, U. Warring, M. Weides, A. C. Wilson, D. J. Wineland, and D. P. Pappas, Rev. Sci. Instrum. **84**, 085001 (2013).

[4]F. Casola, T. van der Sar, and A. Yacoby, Nat. Rev. Mater. **3**, 17088 (2018).

[5]C. Wittneven, R. Dombrowski, M. Morgenstern, and R. Wiesendanger, Phys. Rev. Lett. **81**, 5616 (1998).

[6]R. Dombrowski, C. Steinebach, C. Wittneven, M. Morgenstern, and R. Wiesendanger, Phys. Rev. B **59**, 8043 (1999).

[7]J. Salfi, B. Voisin, A. Tankasala, J. Bocquel, M. Usman, M. Y. Simmons, L. C. L. Hollenberg, R. Rahman, and S. Rogge, Phys. Rev. X **8**, 031049 (2018).

[8]E. Bussmann, M. Rudolph, G. S. Subramania, S. Misra, S. M. Carr, E. Langlois, J. Dominguez, T. Pluym, M. P. Lilly, and M. S. Carroll, Nanotechnology **26**, 085701 (2015).

[9]G. Gramse, A. Kölker, T. Lim, T. J. Z. Stock, H. Solanki, S. R. Schofield, E. Brinciotti, G. Aeppli, F. Kienberger, and N. J. Curson, Sci. Adv. **3**, e1602586 (2017).

[10]J. I. Colless, A. C. Mahoney, J. M. Hornibrook, A. C. Doherty, H. Lu, A. C. Gossard, and D. J. Reilly, Phys. Rev. Lett. **110**, 046805 (2013).

[11]M. Gonzalez-Zalba, S. Barraud, A. Ferguson, and A. Betz, Nat. Commun. **6**, 6084 (2015).

[12]A. Rossi, R. Zhao, A. S. Dzurak, and M. F. Gonzalez-Zalba, Appl. Phys. Lett. **110**, 212101 (2017).

[13]M. Urdampilleta, D. J. Niegemann, E. Chanrion, B. Jadot, C. Spence, P.-A. Mortemousque, C. Bäuerle, L. Hutin, B. Bertrand, S. Barraud, R. Maurand, M. Sanquer, X. Jehl, S. D. Franceschi, M. Vinet, and T. Meunier, "Gate-based high fidelity spin readout in a CMOS device," preprint arXiv:1809.04584 (2018). [cond-mat].

[14]COMSOL AB, www.comsol.com for "COMSOL Multiphysics® v.5.3."

[15]C. H. Yang, A. Rossi, R. Ruskov, N. S. Lai, F. A. Mohiyaddin, S. Lee, C. Tahan, G. Klimeck, A. Morello, and A. S. Dzurak, Nat. Commun. **4**, 2069 (2013).

[16]M. Veldhorst, J. C. C. Hwang, C. H. Yang, A. W. Leenstra, B. de Ronde, J. P. Dehollain, J. T. Muhonen, F. E. Hudson, K. M. Itoh, A. Morello, and A. S. Dzurak, Nat. Nanotechnol. **9**, 981 (2014).

[17]R. Maurand, X. Jehl, D. Kotekar-Patil, A. Corna, H. Bohuslavskyi, R. Laviéville, L. Hutin, S. Barraud, M. Vinet, M. Sanquer, and S. D. Franceschi, Nat. Commun. **7**, 13575 (2016).

[18]M. A. Fogarty, K. W. Chan, B. Hensen, W. Huang, T. Tanttu, C. H. Yang, A. Laucht, M. Veldhorst, F. E. Hudson, K. M. Itoh, D. Culcer, T. D. Ladd, A. Morello, and A. S. Dzurak, Nat. Commun. **9**, 4370 (2018).

[19]E. Kawakami, P. Scarlino, D. R. Ward, F. R. Braakman, D. E. Savage, M. G. Lagally, M. Friesen, S. N. Coppersmith, M. A. Eriksson, and L. M. K. Vandersypen, Nat. Nanotechnol. **9**, 666 (2014).

[20]D. M. Zajac, T. M. Hazard, X. Mi, K. Wang, and J. R. Petta, Appl. Phys. Lett. **106**, 223507 (2015).

[21]D. V. Averin, A. B. Zorin, and K. K. Likharev, Sov. Phys. JETP **61**, 407 (1985).

[22]T. Duty, G. Johansson, K. Bladh, D. Gunnarsson, C. Wilson, and P. Delsing, Phys. Rev. Lett. **95**, 206807 (2005).

[23]M. A. Sillanpää, T. Lehtinen, A. Paila, Y. Makhlin, L. Roschier, and P. J. Hakonen, Phys. Rev. Lett. **95**, 206806 (2005).

[24]K. D. Petersson, C. G. Smith, D. Anderson, P. Atkinson, G. A. C. Jones, and D. A. Ritchie, Nano Lett. **10**, 2789 (2010).

[25]A. Cottet, C. Mora, and T. Kontos, Phys. Rev. B **83**, 121311(R) (2011).

[26]R. Mizuta, R. M. Otxoa, A. C. Betz, and M. F. Gonzalez-Zalba, Phys. Rev. B **95**, 045414 (2017).

[27]R. Ruskov and C. Tahan, "Quantum-limited measurement of spin qubits via curvature coupling to a cavity," preprint arXiv:1704.05876v1 (2017). [cond-mat].

[28]Y.-P. Shim and C. Tahan, Phys. Rev. B **97**, 155402 (2018).

[29]N. Samkharadze, G. Zheng, N. Kalhor, D. Brousse, A. Sammak, U. C. Mendes, A. Blais, G. Scappucci, and L. M. K. Vandersypen, Science **359**, 1123 (2018).

[30]X. Hao, R. Ruskov, M. Xiao, C. Tahan, and H. Jiang, Nat. Commun. **5**, 3860 (2014).

[31]J. K. Gamble, M. A. Eriksson, S. N. Coppersmith, and M. Friesen, Phys. Rev. B **88**, 035310 (2013).

[32]R. Ruskov, M. Veldhorst, A. S. Dzurak, and C. Tahan, Phys. Rev. B **98**, 245424 (2018).

[33]G. Burkard and J. R. Petta, Phys. Rev. B **94**, 195305 (2016).

[34]S. E. de Graaf, A. V. Danilov, A. Adamyan, and S. E. Kubatkin, Rev. Sci. Instrum. **84**, 023706 (2013).